Supporting Information

Synthesis, Preclinical Evaluation and Molecular Modelling of Macrocyclic Appended 1-(2-methoxyphenyl)piperazine for 5-HT1A Neuroreceptor Imaging

Puja Panwar Hazari[a], Surbhi Prakash[a,b], Virendra Kumar Meena[a,b], Niraj Singh[a], Krishna Chuttani[a], Nidhi Chadha[a], Pooja Singh[a,b], Shrikant Kukreti[b] and Anil Kumar Mishra[a*]

[a]Division of Cyclotron and Radiopharmaceutical Sciences, Institute of Nuclear Medicine and Allied Sciences, Brig SK Mazumdar Road, Delhi-110054, India.

[b]Department of Chemistry, University of Delhi, Delhi-110007, India.

Supporting Information Description:

Characterization data

Fig. S1 ^{1}H NMR spectrum of 2-chloro-N-(4-(4-(2-methoxyphenyl)piperazin-1-yl)butylacetamide **(3)**

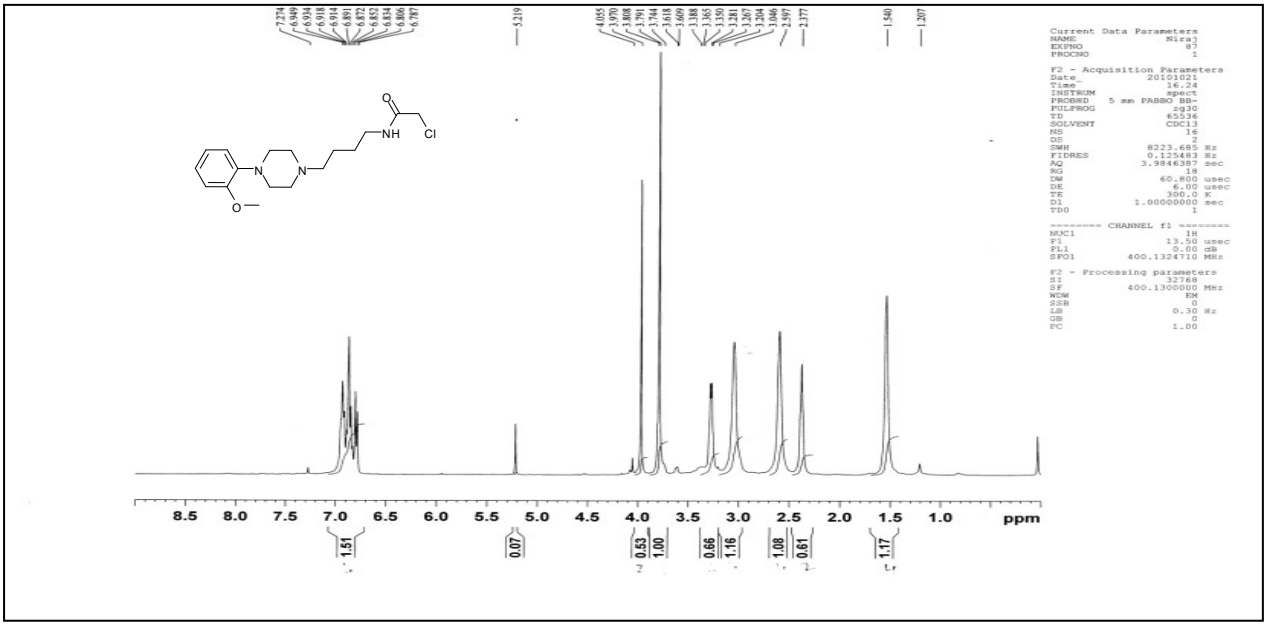

Fig. S2 ^{13}C NMR spectrum of 2-chloro-N-(4-(4-(2-methoxyphenyl)piperazin-1-yl)butylacetamide **(3)**

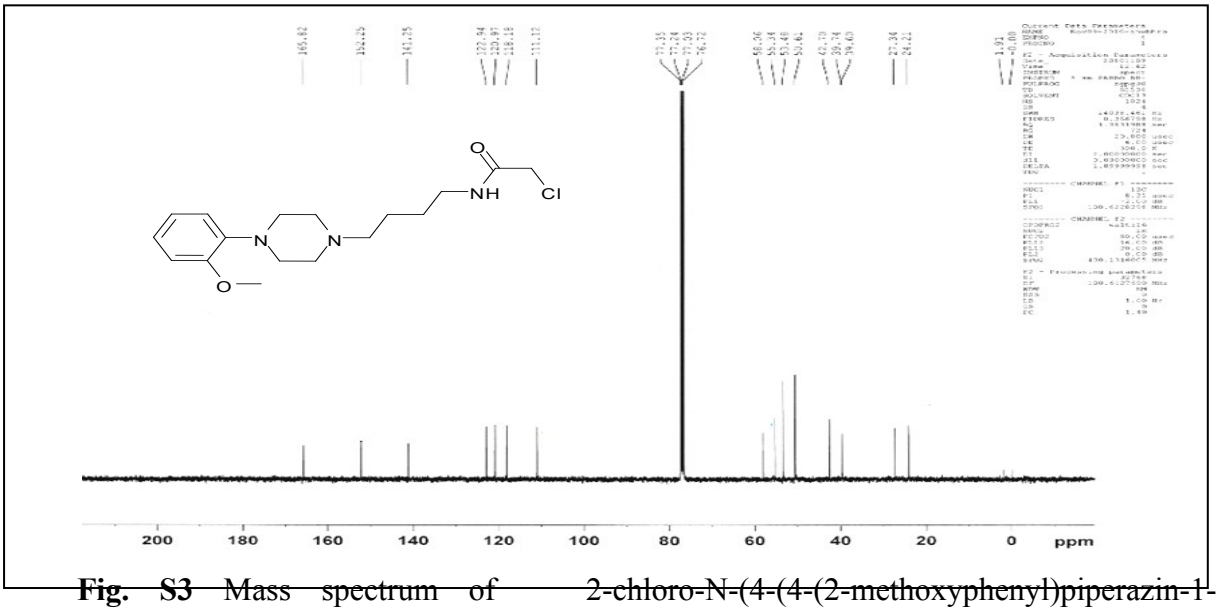

Fig. S3 Mass spectrum of 2-chloro-N-(4-(4-(2-methoxyphenyl)piperazin-1-yl)butylacetamide **(3)**

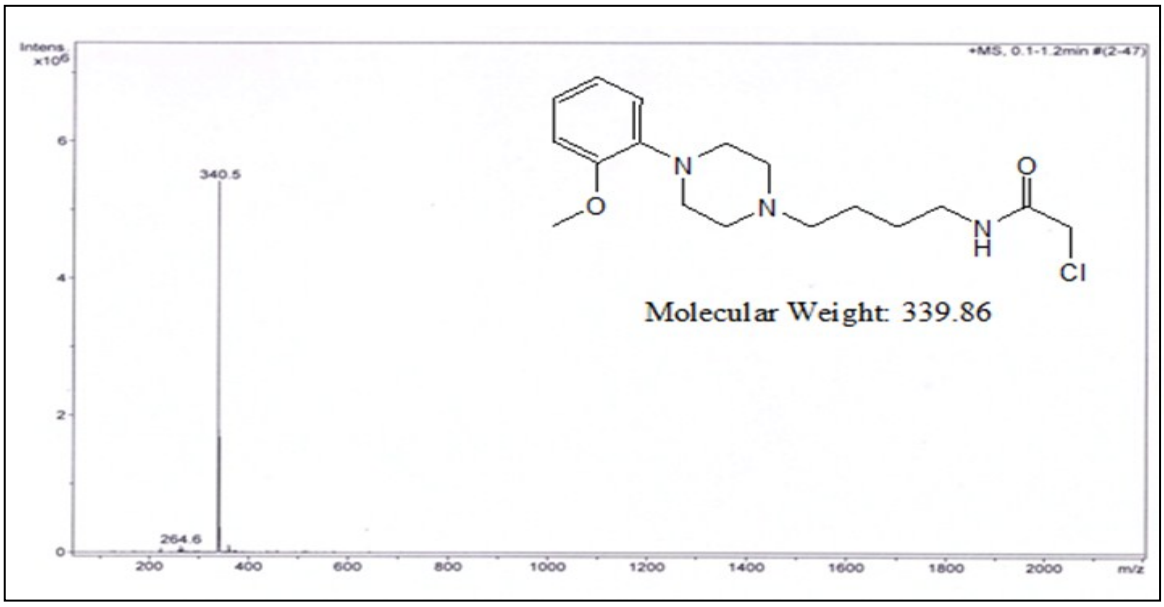

Fig. S4 ^{1}H NMR spectrum of (4,7-bis-*t*-butoxycarbonylmethyl-1,4,7,10 tetraaza-cyclododec-1-yl)-acetic acid *t*-butyl ester **(4)**

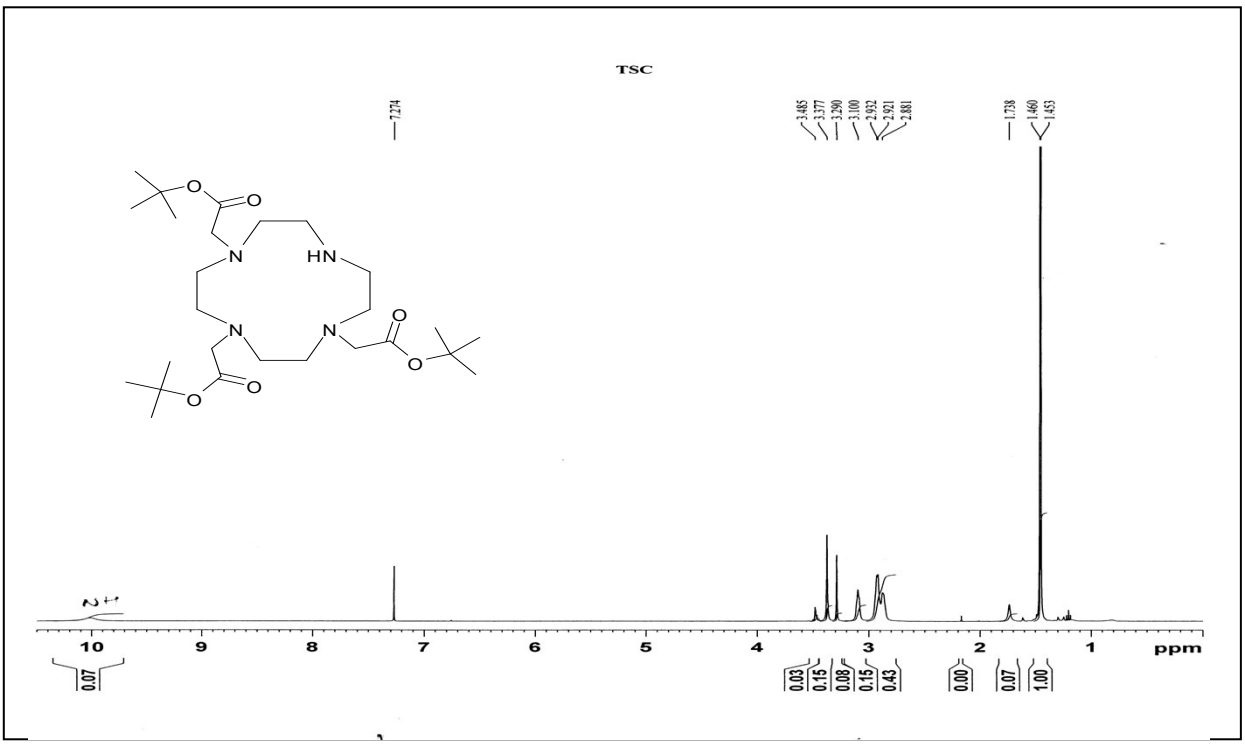

Fig. S5 ^{13}C NMR spectrum of (4,7-bis-*t*-butoxycarbonylmethyl-1,4,7,10 tetraaza-cyclododec-1-yl)-acetic acid *t*-butyl ester **(4)**

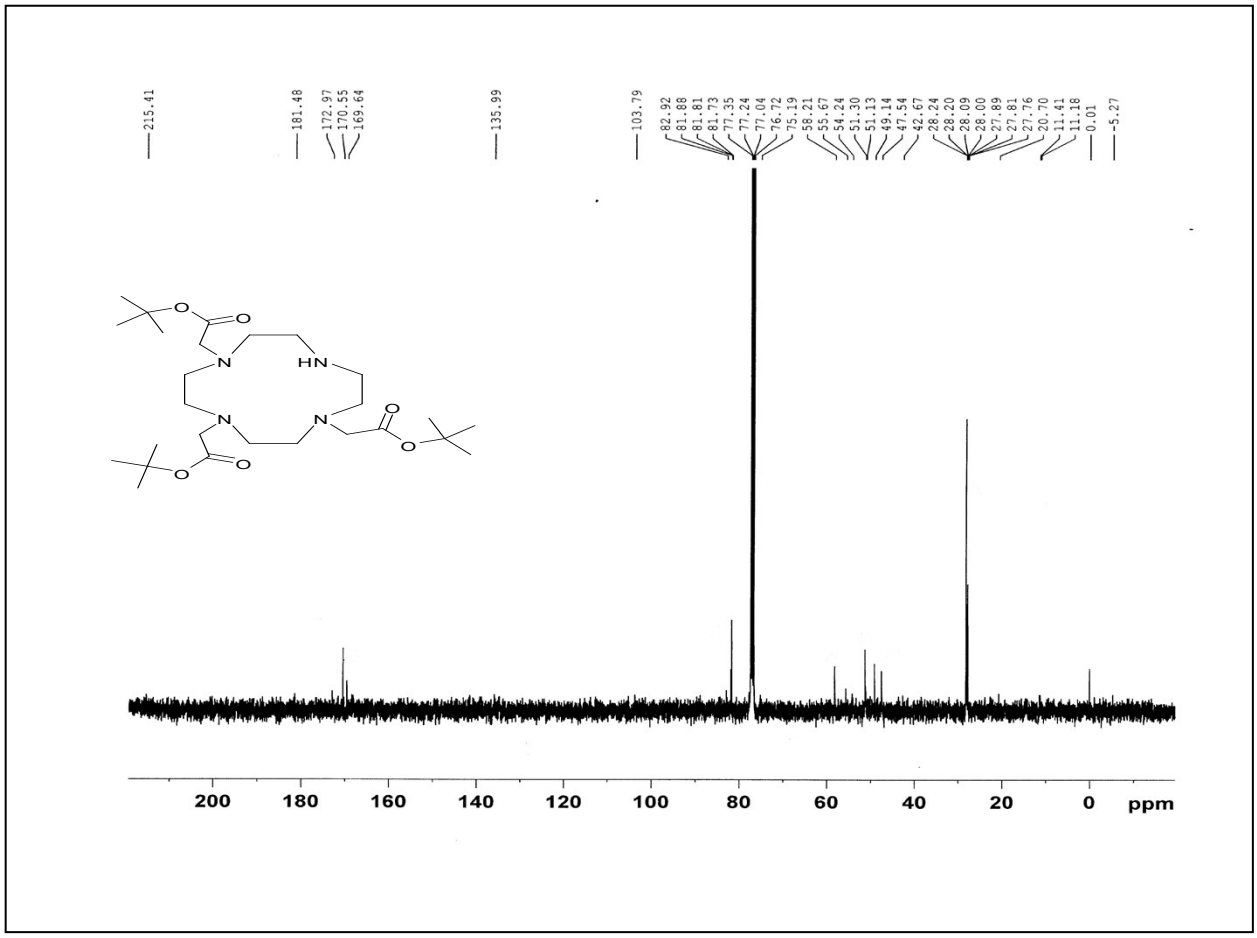

Fig. S6 Mass spectrum of (4,7-bis-*t*-butoxycarbonylmethyl-1,4,7,10 tetraaza-cyclododec-1-yl)-acetic acid *t*-butyl ester **(4)**

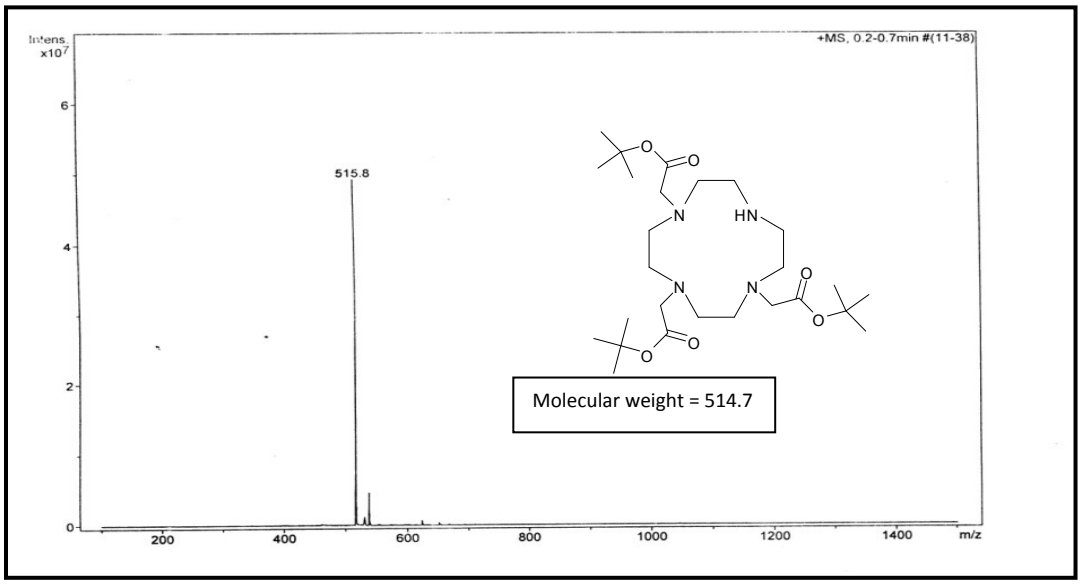

Fig. S7 ^{1}H NMR spectrum of tert-butyl 2,2',2''-(10-(2-(4-(4-(2-methoxyphenyl)piperazin-1-yl)butylamino)-2-oxoethyl)-1,4,7,10-tetraazacyclododecane-1,4,7-triyl)triacetate **(5)**

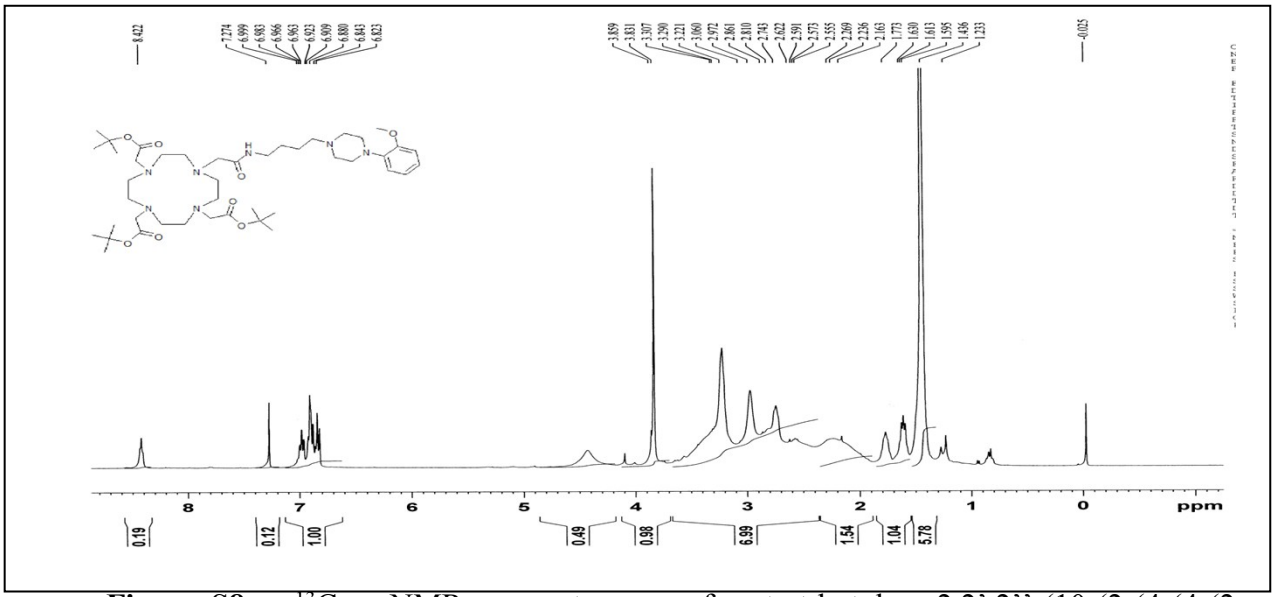

Fig. S8 ^{13}C NMR spectrum of tert-butyl 2,2',2''-(10-(2-(4-(4-(2-methoxyphenyl)piperazin-1-yl)butylamino)-2-oxoethyl)-1,4,7,10-tetraazacyclododecane-1,4,7-triyl)triacetate **(5**

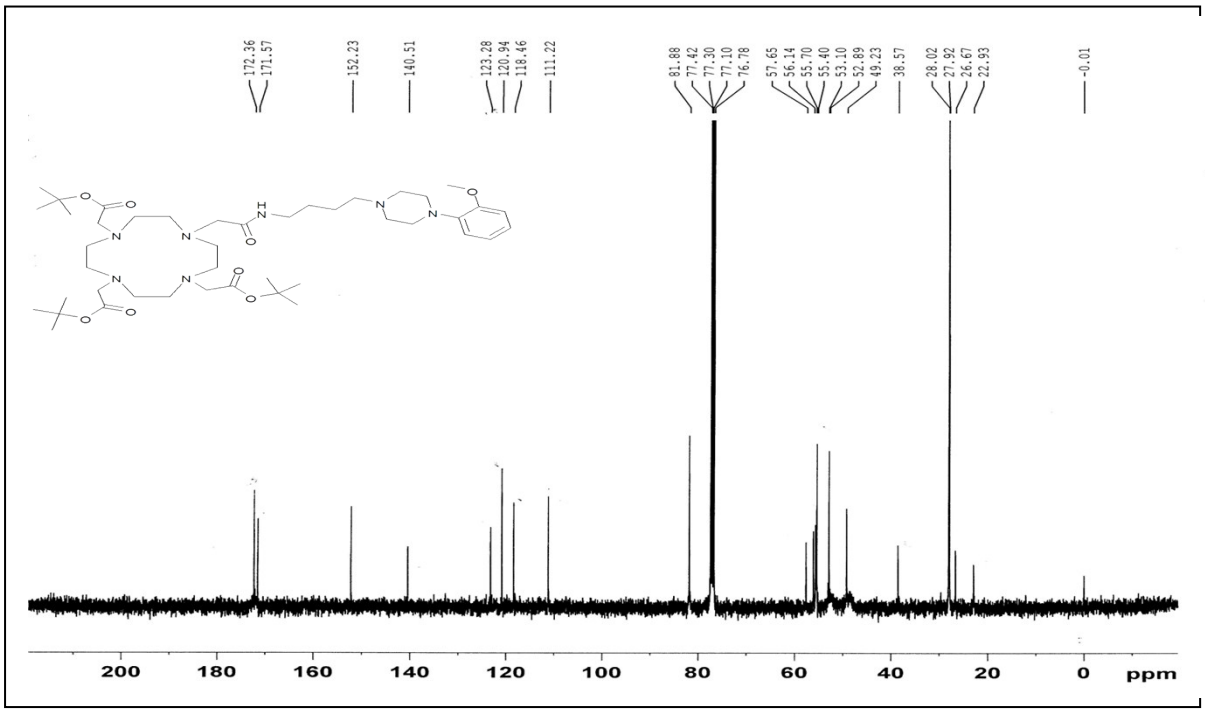

Fig. S9 ESI and HRMS of tert-butyl 2,2',2''-(10-(2-(4-(4-(2-methoxyphenyl)piperazin-1-yl)butylamino)-2-oxoethyl)-1,4,7,10-tetraazacyclododecane-1,4,7-triyl)triacetate **(5)**

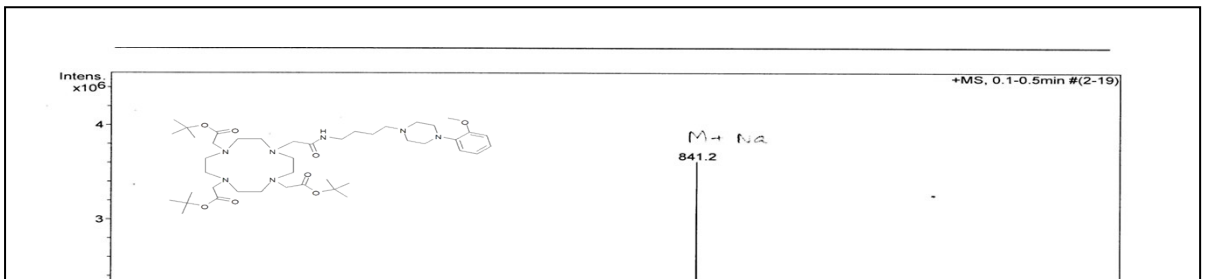

Molecular weight = 818.1

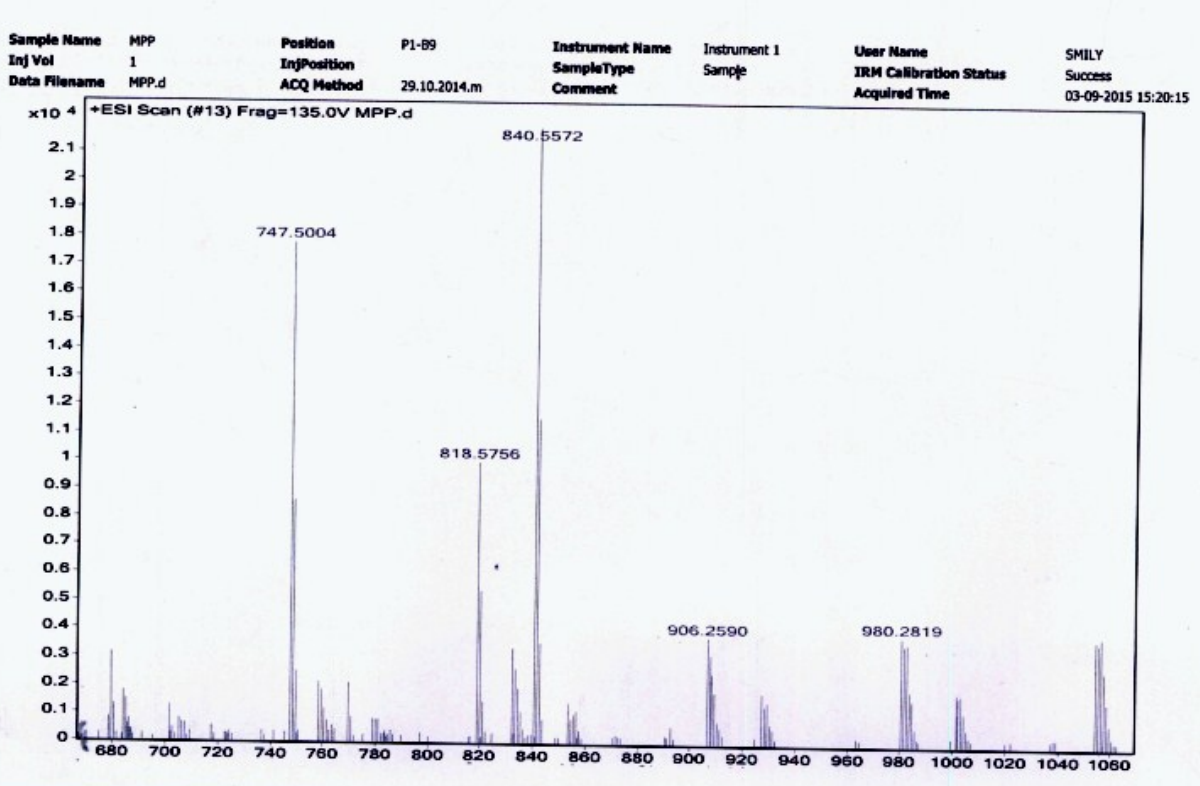

Fig. S10 ^{1}H NMR Spectrum of 2,2',2''-(10-(2-(4-(4-(2-methoxyphenyl)piperazin-1-yl)butylamino)-2-oxoethyl)-1,4,7,10-tetraazacyclododecane-1,4,7-triyl)triacetic acid **(6)**

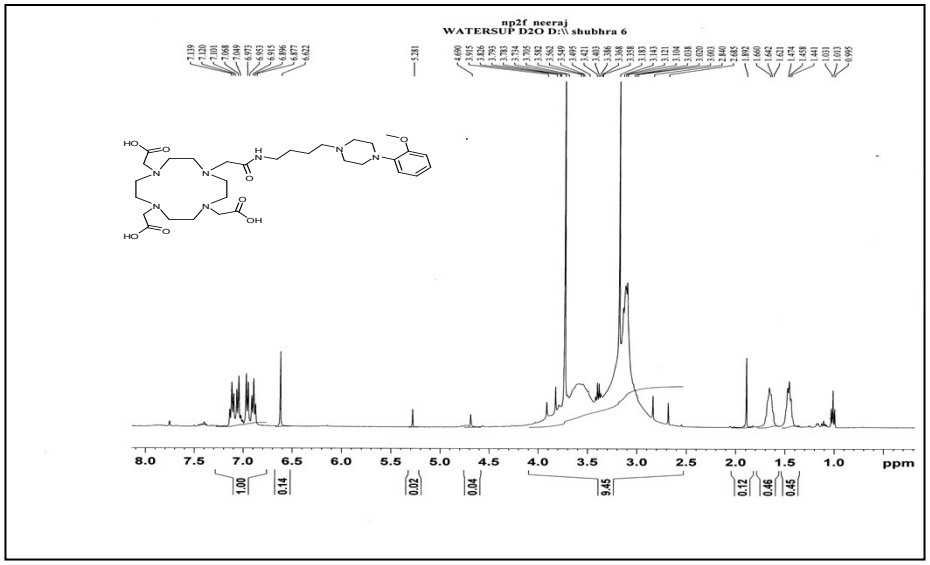

Fig. S11 ^{13}C NMR spectrum of 2,2',2''-(10-(2-(4-(4-(2-methoxyphenyl)piperazin-1yl)butylamino)-2-oxoethyl)-1,4,7,10-tetraazacyclododecane-1,4,7-triyl)triacetic acid

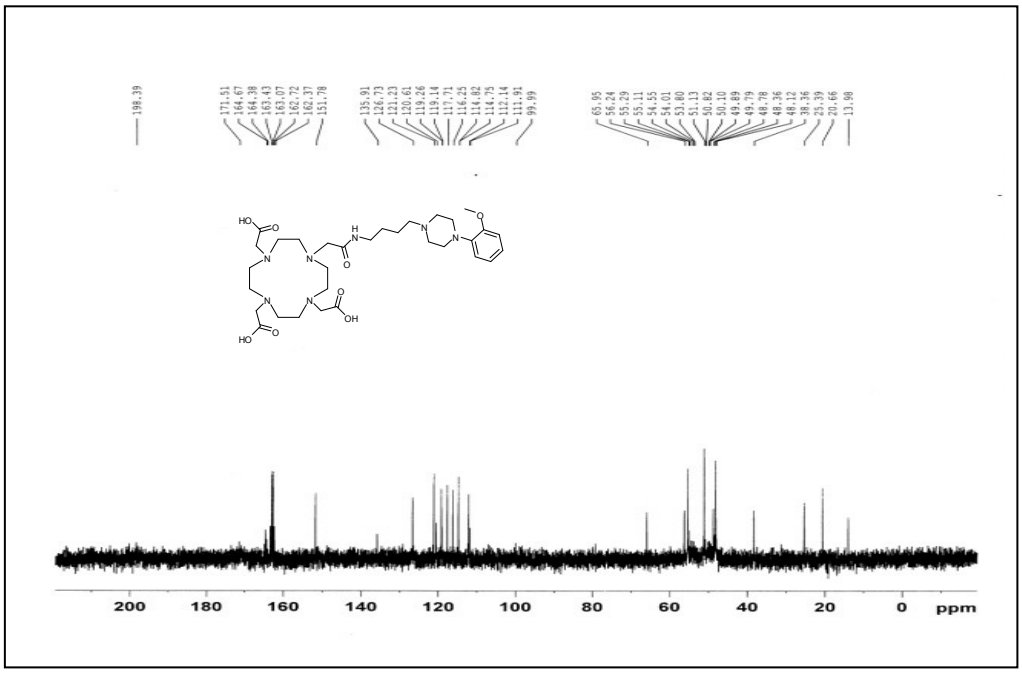

Fig. S12 ESI and HRMS of 2,2',2''-(10-(2-(4-(4-(2-methoxyphenyl)piperazin-1yl)butylamino)-2-oxoethyl)-1,4,7,10-tetraazacyclododecane-1,4,7-triyl)triacetic acid **(6)**

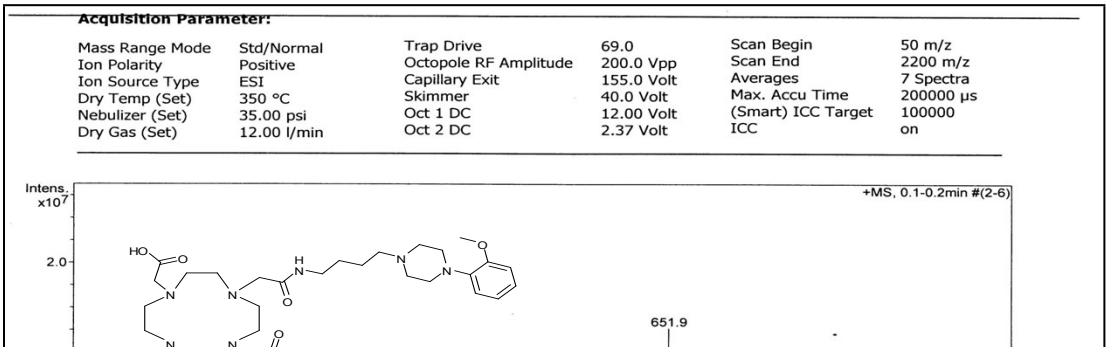

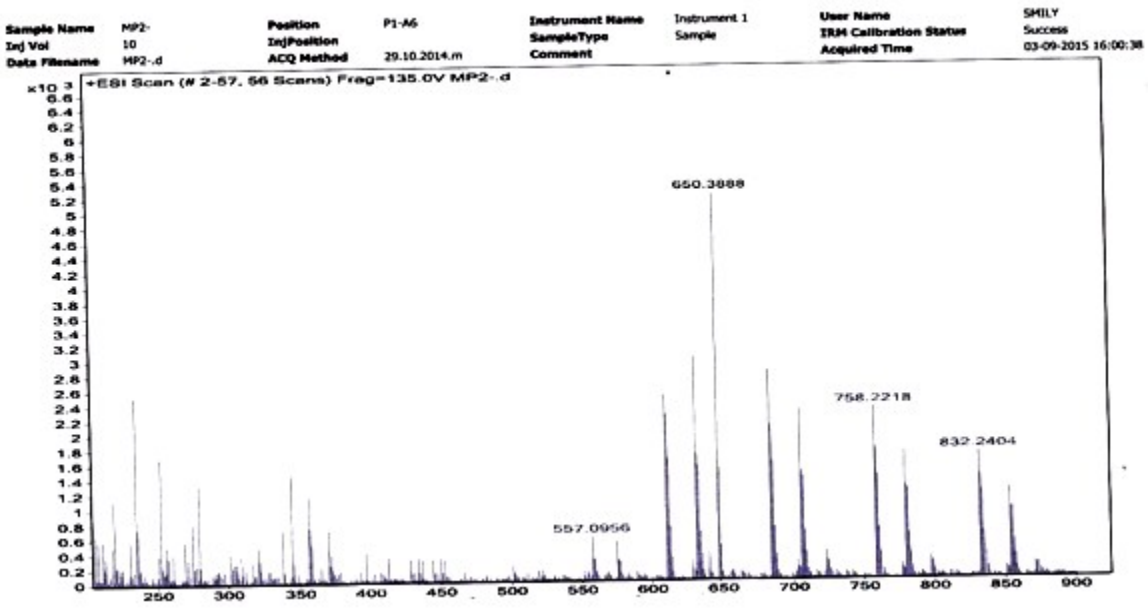
Sample Name MP2-
Inj Vol 10
Data Filename MP2-.d
Position P1-A6
InjPosition
ACQ Method 29.10.2014.m
Instrument Name Instrument 1
SampleType Sample
Comment
User Name SHILY
IRM Calibration Status Success
Acquired Time 03-09-2015 16:00:38
+ESI Scan (# 2-57, 56 Scans) Frag=135.0V MP2-.d
x10 3
650.3888
758.2218
832.2404
557.0956
250 300 350 400 450 500 550 600 650 700 750 800 850 900

Fig. S13 Mass spectrum of Ga(III) complex of DO3A-butyl-MPP

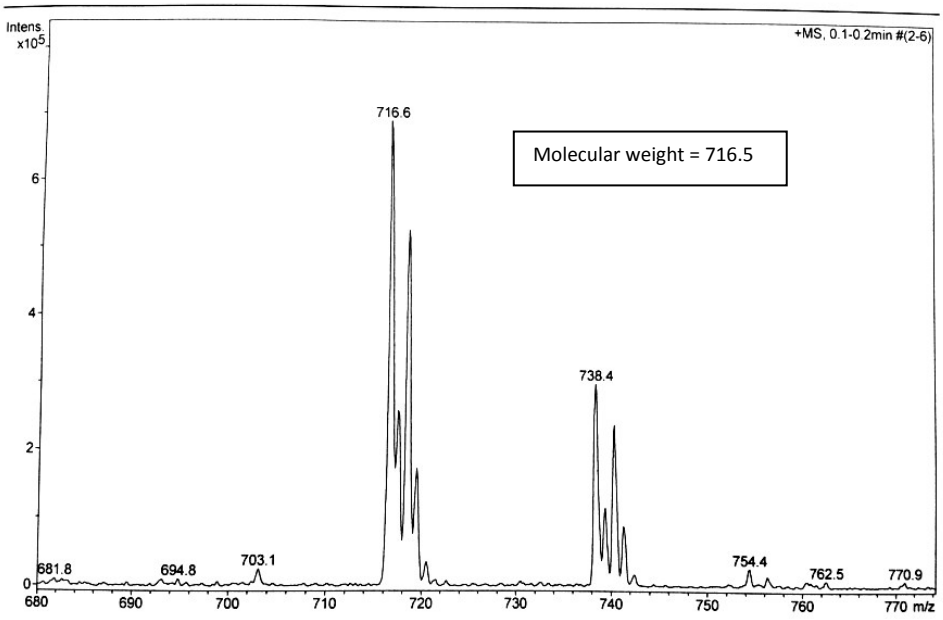

Fig. S14 HRMS of *Ga-DO3A-butyl-MPP(MW:715.2820 Found M^+at 713.0644, $(M+2Na)^+$at 758.2190*

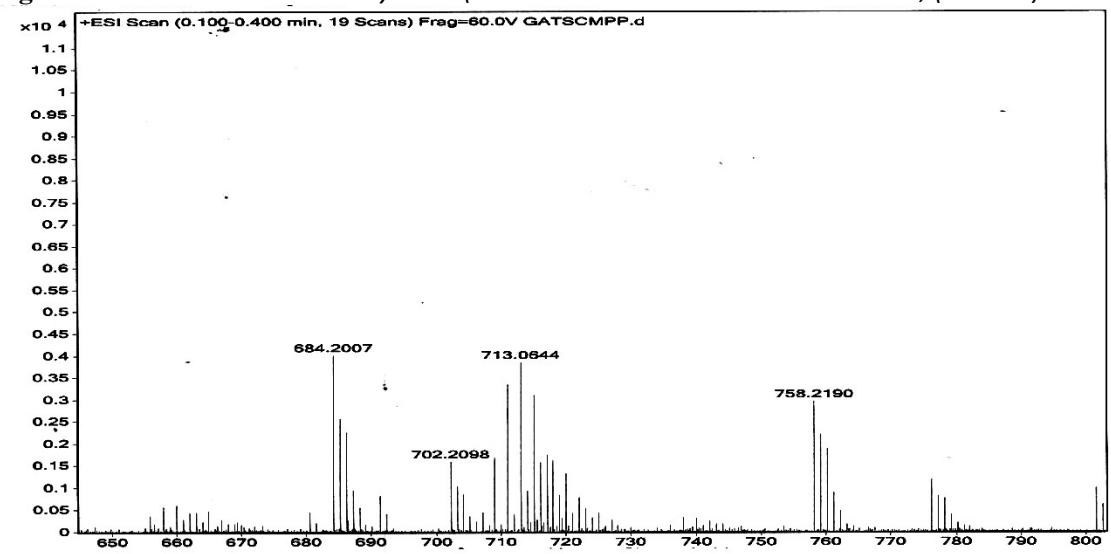

Fig. S15 Mass spectrum of Gd(III) complex of DO3A-butyl-MPP

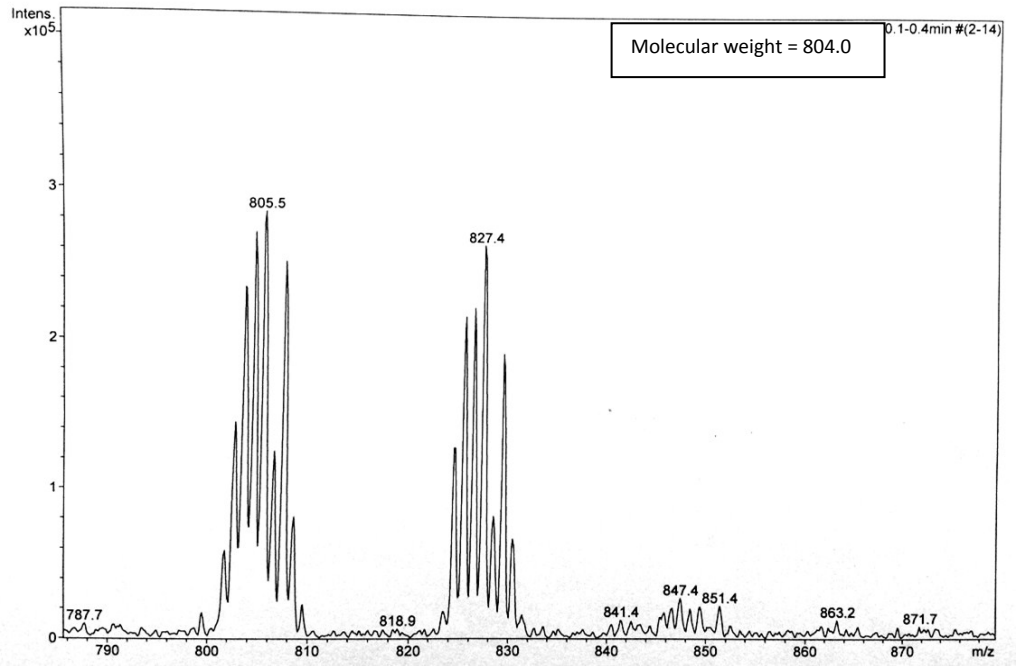

Fig. S16 HRMS of Gd-DO3A-butyl-MPP(MW:804.2805) Found $(M+H)^+$at 805.2805, $(M+Na)^+$ at 822.270

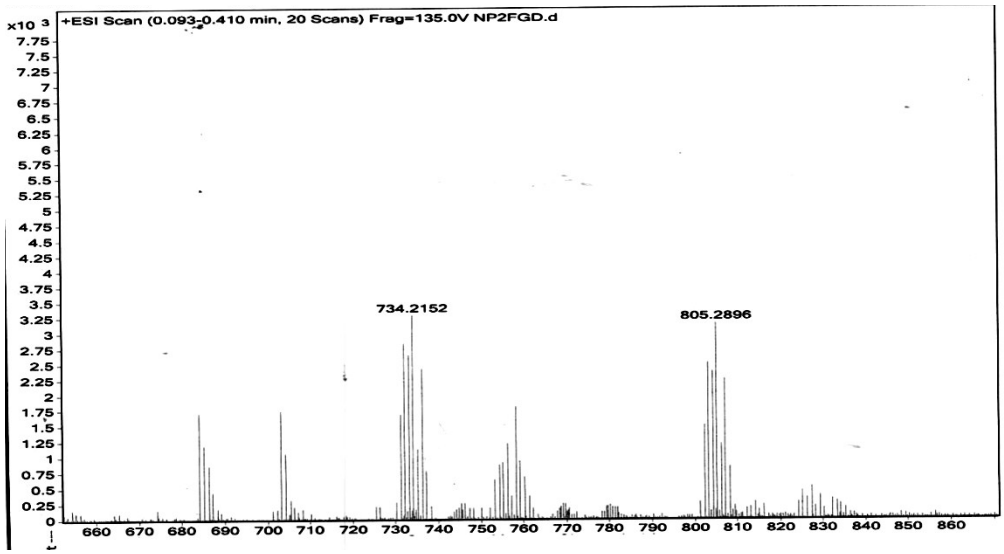

Fig. S17 Mass spectrum of Eu(III) complex of DO3A-butyl-MPP

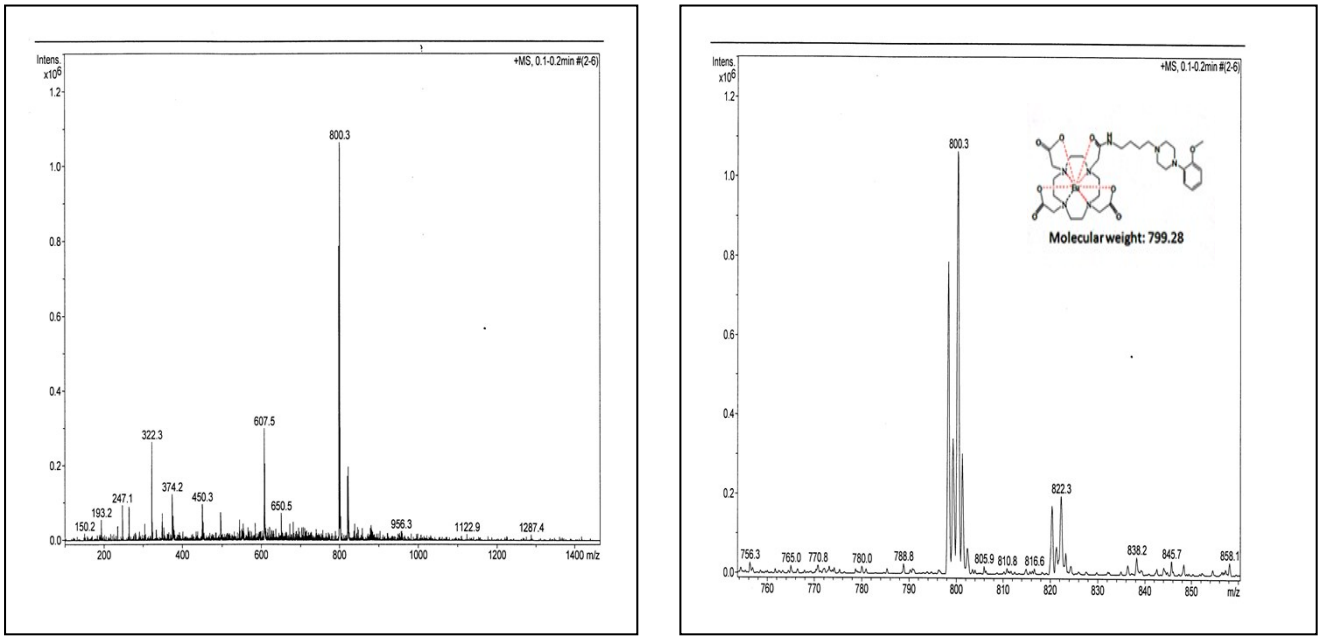

Fig. S18 HRMS of *Eu-DO3A-butyl-MPP(MW:799.2777) Found (M+1)at 800.2840, (M+Na)at 822.2700*

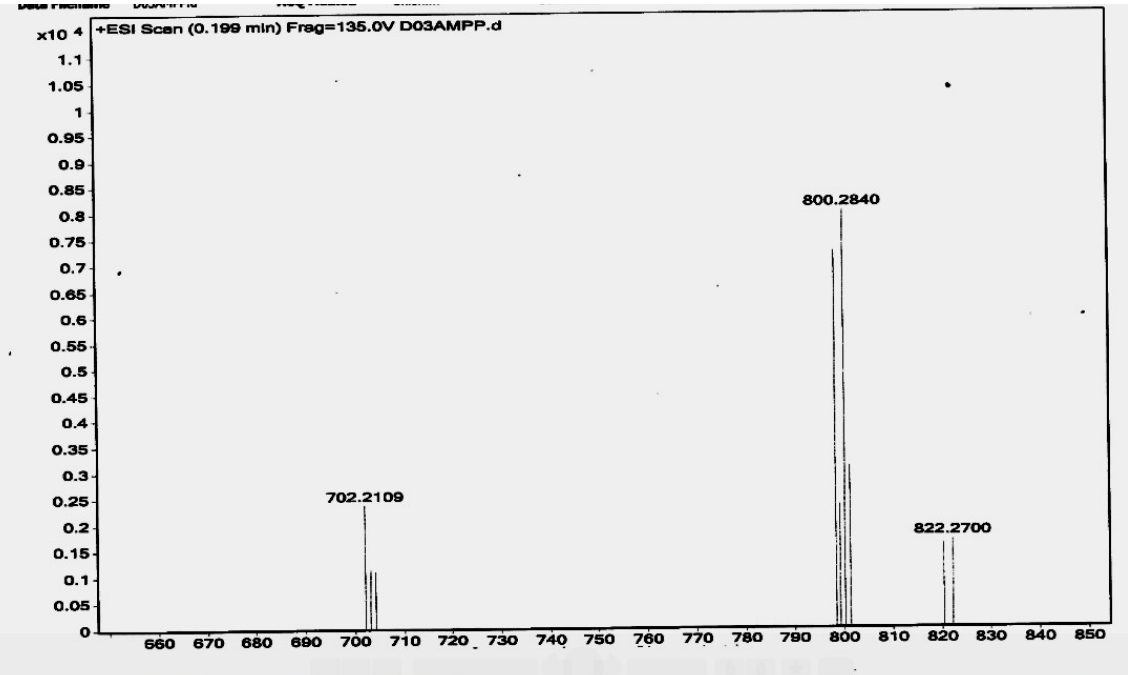

S19 Calibration curves of cold Ga-DO3AMPP and Calculation of Specific Activity

Fig. S19(A) Calibration Curve of Ga-DO3AMPP

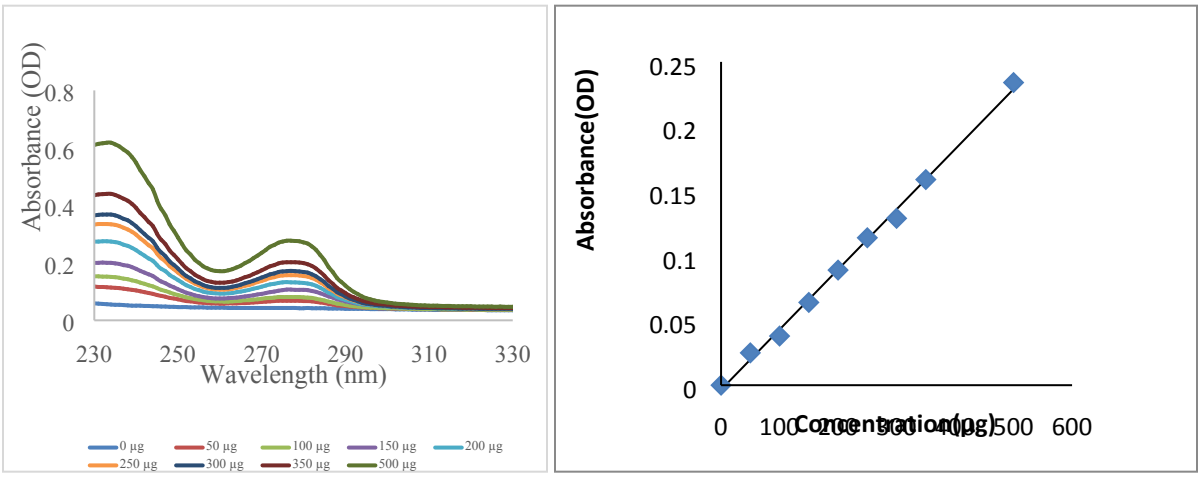

Absorbance spectra were taken at different concentrations in spectrophotometer (Synergy H4 Hybrid microplate reader from Biotek) ranging from 10 to 500µg, absorbance maxima was found to be 277nm. The calibration curve thus obtained was used to find concentrations of samples depending on their absorbance. Graph plotted for the same is also shown.

Details of Analytical HPLC

Analytical HPLC was performed on Atlantis T3C-18 reverse-phase column (5 µm, 4.6 mm x 250 mm) using Agilent1260 Infinity Analytical-Scale Purification System. The mobile phase was 0.05 % TFA in water (solvent A) and methanol (solvent B) with a flow rate of 0.8 mL/min. Gradient 0%-20% solvent B in 20 min. UV detection was performed at 277 nm using a UV-Vis detector. Effective Concentration ranging from 0.0156µg/µL-1µg/µL was taken with Injection volume of 10 µL. Retention time was found to be 5.8 min.

Analytical HPLC profile for 10 µg concentration of compound

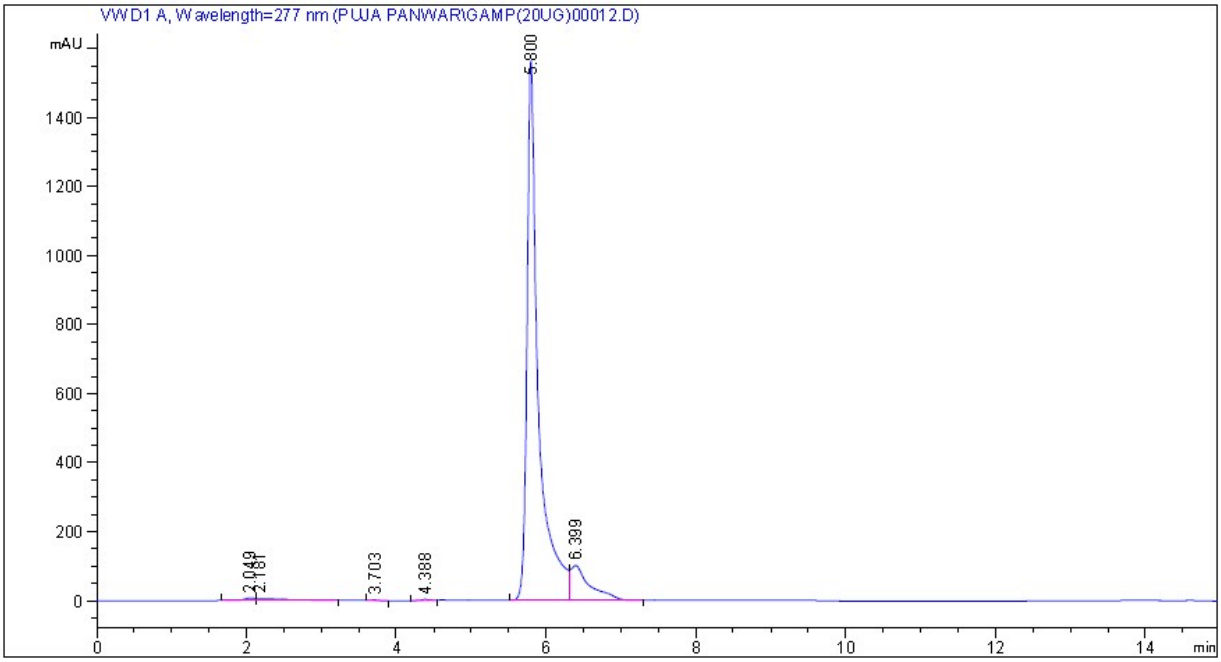

Peak #	RetTime [min]	Type	Width [min]	Area [mAU*s]	Height [mAU]	Area %
4	4.388	BV	0.1185	27.67426	3.19725	0.1487
5	5.800	BV	0.1477	1.64878e4	1564.49951	88.5696
6	6.399	VB	0.2497	1866.30664	100.74429	10.0255
Totals :				1.86156e4	1682.70075	

Calculation of Specific Activity

Decay corrected product radioactivity was measured after the end of synthesis and purification at 15 min. Radiolabeling was started with 200 µg of compound as analysed through Synergy Hybrid Spectrophotometer. After radiolabeling the compound with ^{68}Ga, the reaction mixture was passed through sepak and elution was done with 1mL of ethanol. This ethanolic solution was concentrated and 40 µL water was added to it. From this 10 µL was injected into analytical HPLC to deduce the amount of the radiopharmaceutical. Calibration curve of cold Ga complex has been provided below.

Fig. S19(B) Calibration Curve of cold Ga-DO3AMPP derived from Analytical HPLC

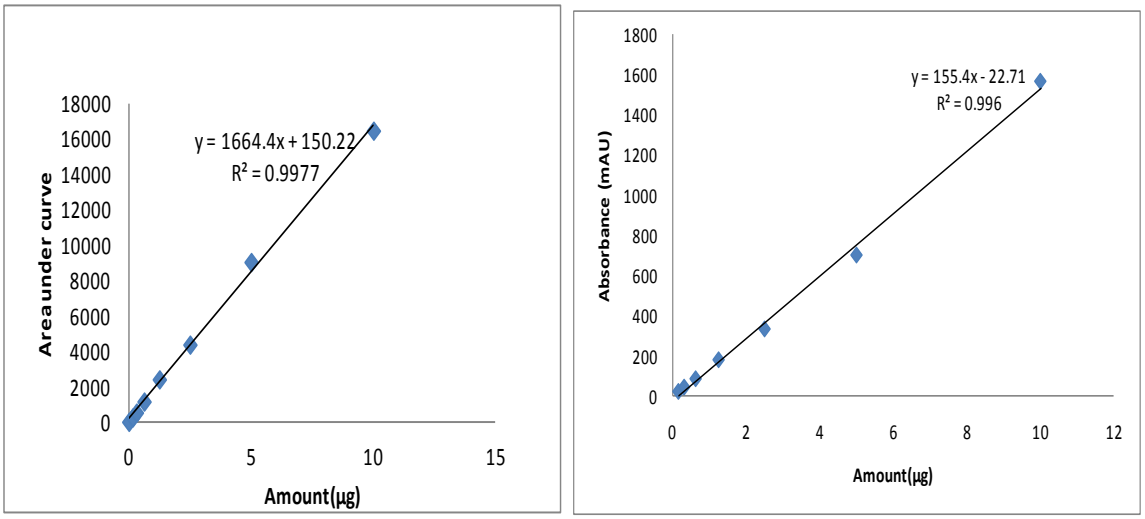

Concentration(µg)	Area of peak (mAU*s)	Height of peak(mAU)
10 µg	1.648×10^4	1564.49
5 µg	9046.3027	700
2.5 µg	4371.3892	332.366
1.25	2405.1145	179.10342
0.625 µg	1150.1252	84.5997
0.3125 µg	525.80	42.9015
o.156 µg	250.754	21.4332

An absorbance of 21.976 and area under curve of 252.3 obtained during analytical HPLC showed a concentration of 0.16 µg in 10 µL which make final amount to 0.64 µg in 40 µL volume of concentrate as deduced from the equation. Peak was collected and the radioactivity associated with it (12.78 mCi) was counted and accordingly specific activity (A_S) was calculated and found to be 529.08 GBq/ µmol.

Fig. S20 Chromatograms of the ^{68}Ga-DO3A-butyl-MPP and ^{68}Ga-Acetate.

EZTLC Scan

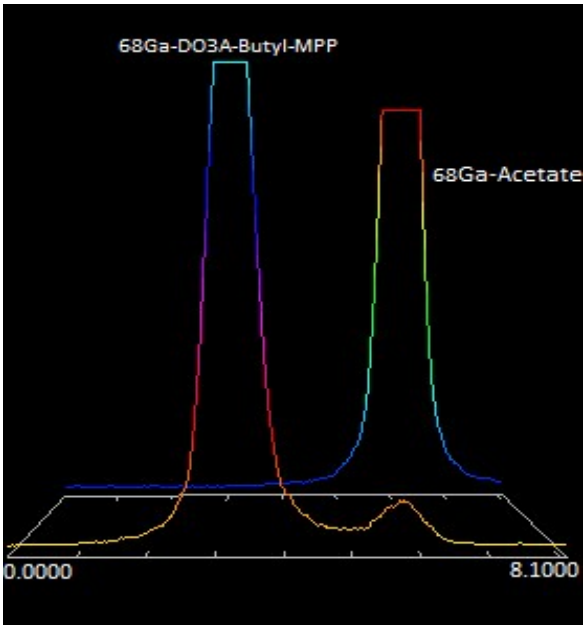

RadioHPLC of ^{68}Ga-DO3A-butyl-MPP

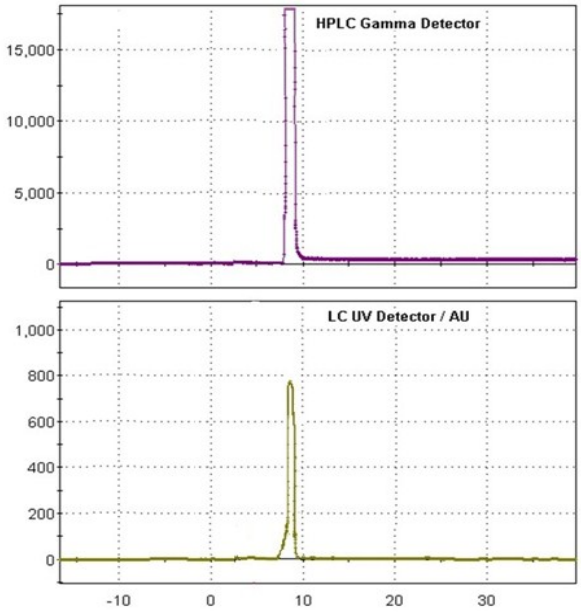

Coelution of ^{68}Ga-DO3A-butyl-MPP and Ga(III)-DO3A-butyl-MPP complexes.

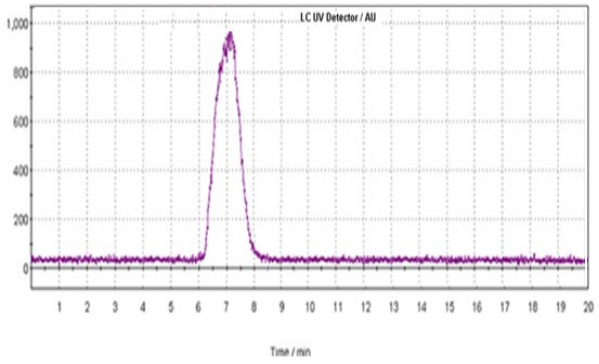

Fig S21 Optimization of Radiolabeling with respect to heating time, pH, precursor amount used and temperature.

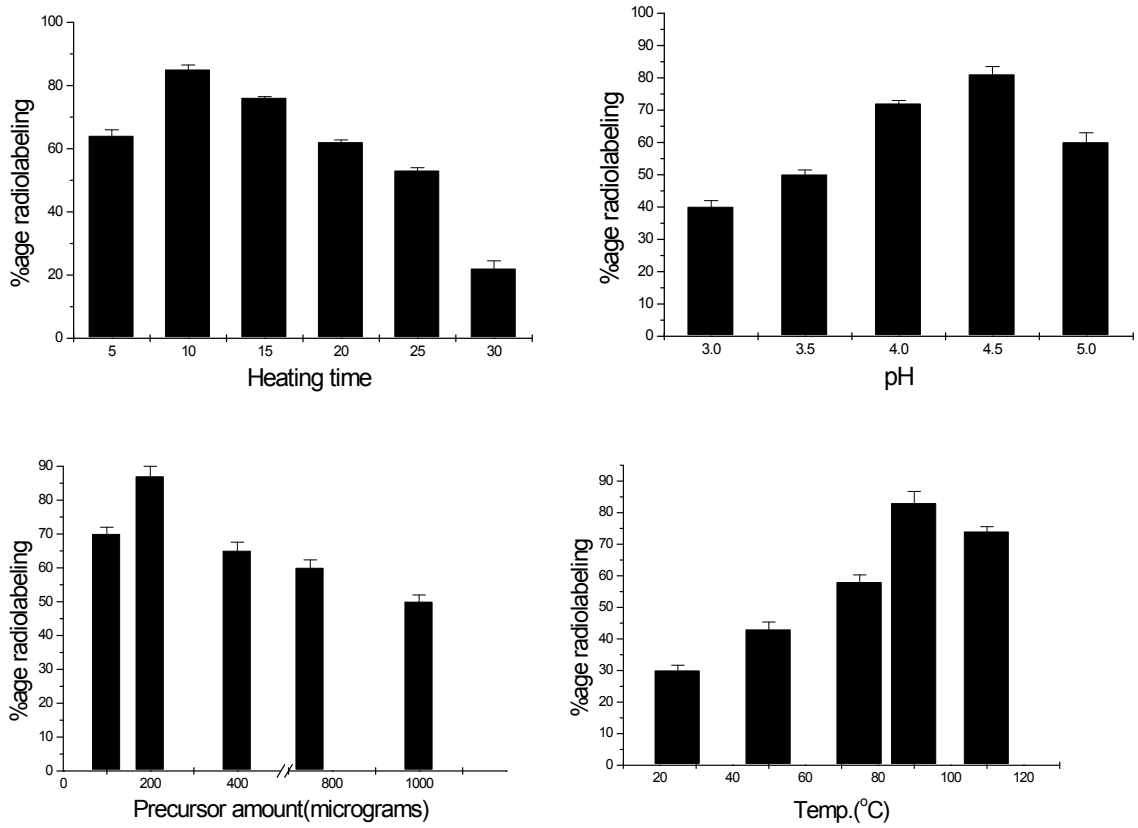

Fig S22. Human Serum Stability Assay

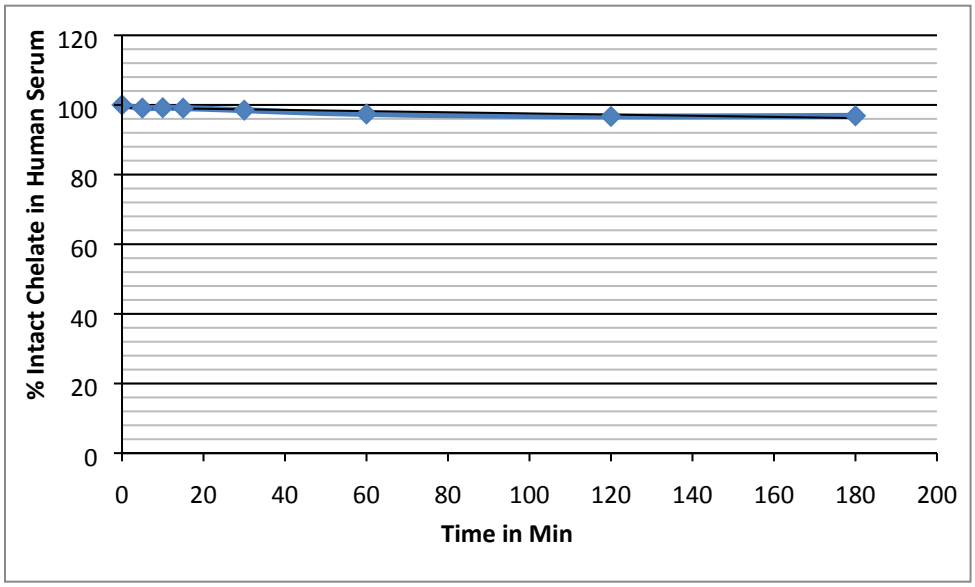

Fig S23. A) Cytotoxicity of DO3A-butyl-MPP (MTT Assay) in *HEK cells* (0.001-10 mM concentration range).

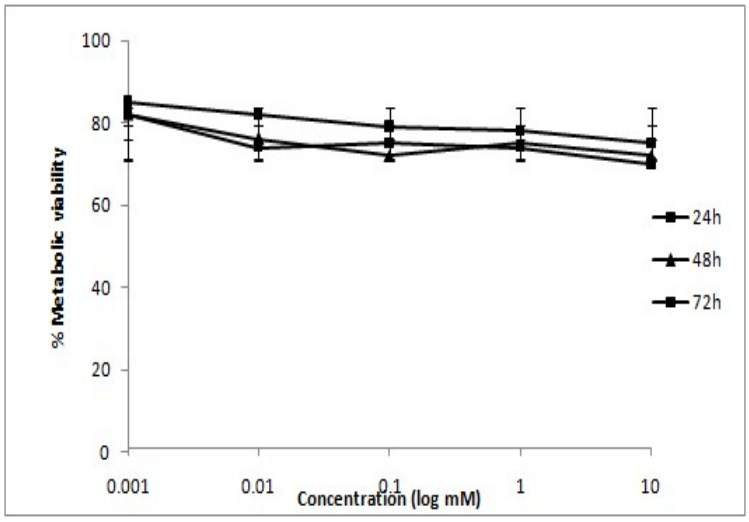

B) Scatchard plot of the specific binding data to the ratio of bound to free (B/F) for primary hippocampal cells for DO3A-butyl-MPP

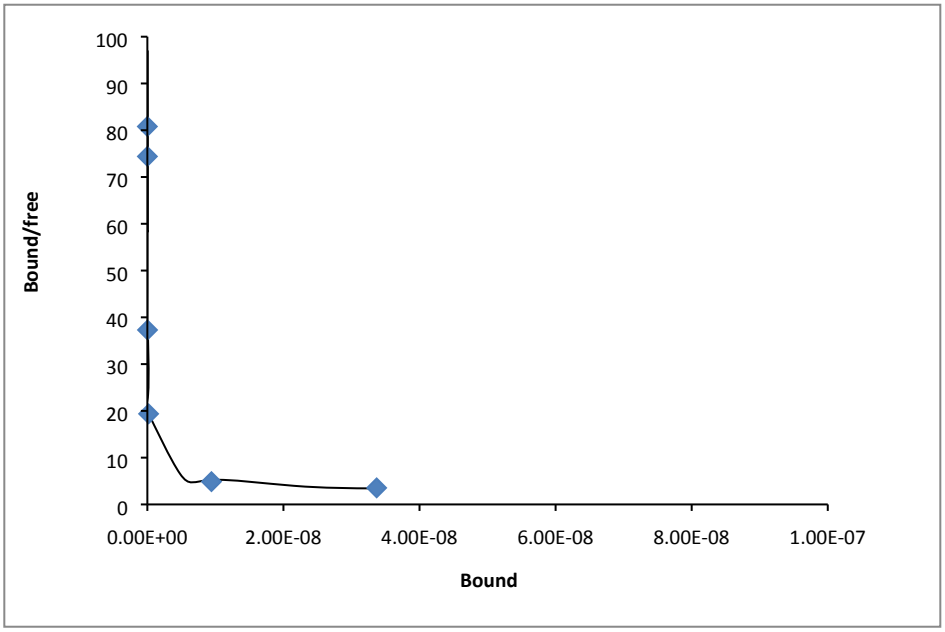

Fig S24. Scatchard plot of the Radioligand binding assay on A) 5HT1A B) 5HTT and C) 5HT2A brain homogenate

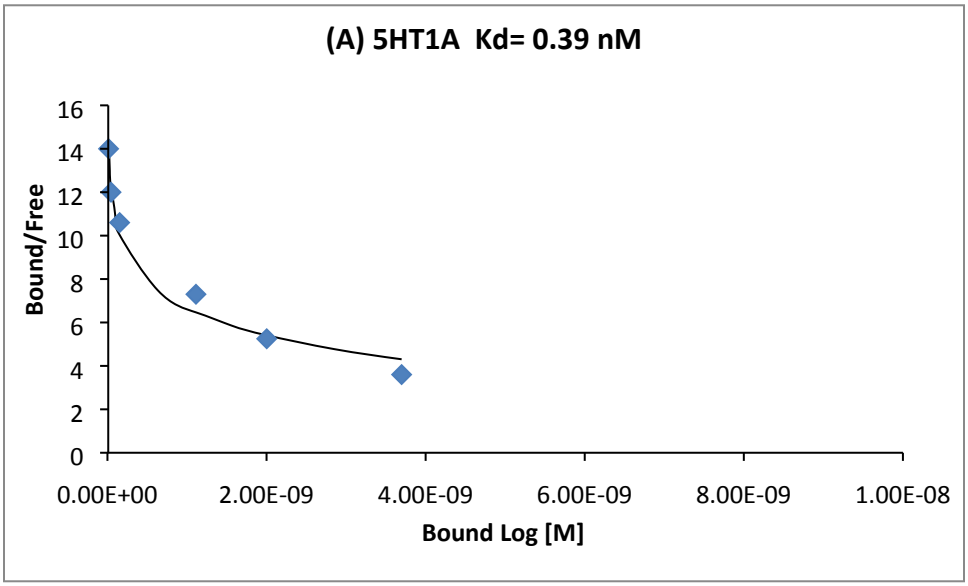

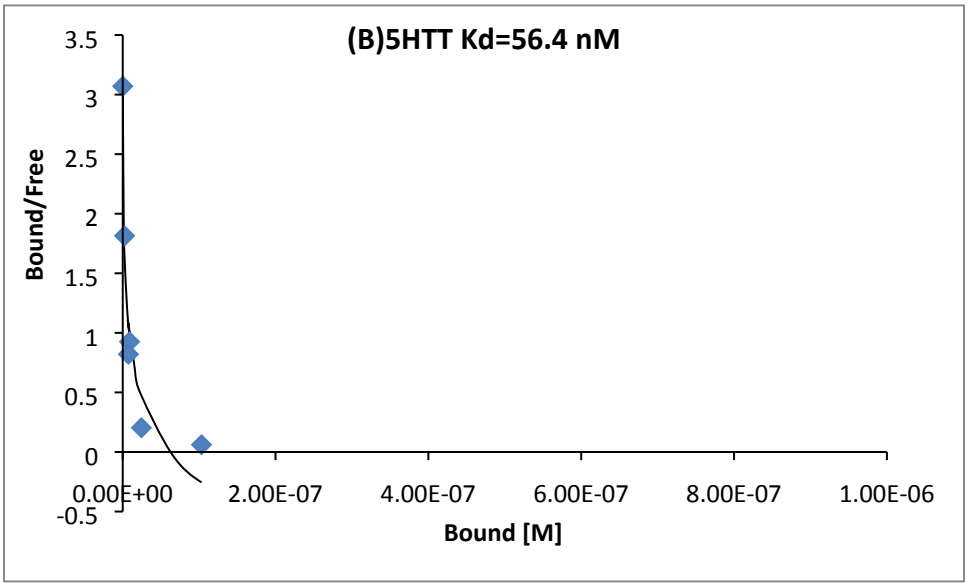

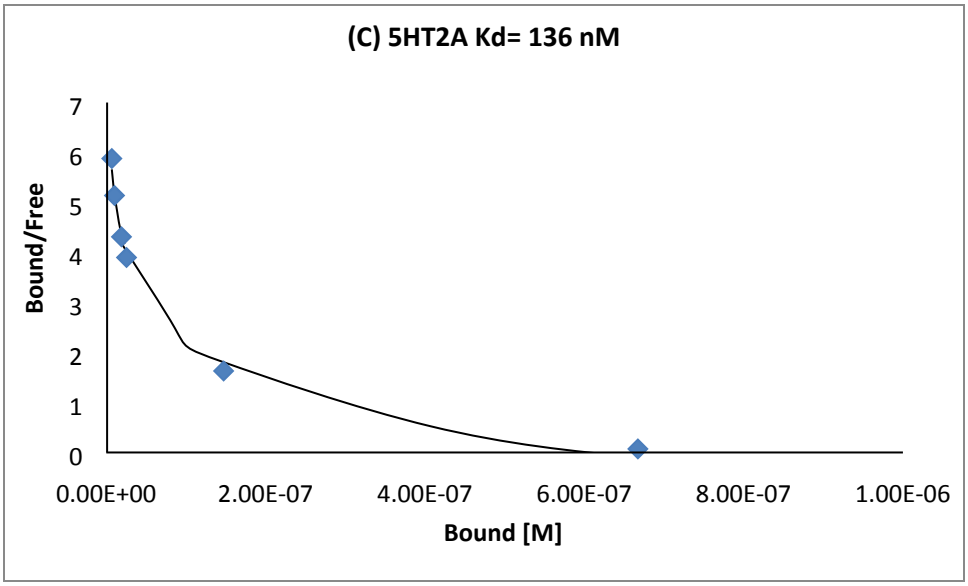

S24. Molecular modeling and docking studies with monomeric 5-HT$_{1A}$ receptor models:

Homology modeling and flexible docking studies has been performed for DO3A-butyl-MPP with human 5-HT$_{1A}$ homology modeled receptor. In case of human 5-HT$_{1A}$ receptor, sequence similarity (~48%) with human β_2-adrenergic receptor in the transmembrane region is considerably higher compared to the similarity (~38%) between 5-HT$_{1A}$ receptor and rhodopsin sequences. The homology model was generated using the 2RH1 crystal structure of the β_2 GPCR as the template for homology modeling of the 5-HT$_{1A}$ receptor. Earlier models were built by using rhodopsin as a template, but after the release of 2RH1, many GPCRs are reported due to the high similarity of structural and functional relationships between the template and the modeled protein. The crystal structure of 2RH1 has been reported at highest resolution of 2.4Å among all the available GPCR crystal structures including β_1 structure with which it has high similarity. The β_2 crystal structure contains structural information for the extracellular side of the receptor, near the binding site.

The 5-HT$_{1A}$ model was generated on 2RH1 as template due to fair sequence alignment of ~48% amino acid similarity in conserved transmembrane (TM) region of β_2-adrenergic receptor and 5-HT$_{1A}$ sequence. The 5-HT$_{1A}$ model was optimized; refined and Ramachandran plot validates the models where residues are present in allowed region without any steric clashes. The reliable modeling of TM region is important since ligand binding pockets lies in TM region of the 5-HT$_{1A}$ monomer. The 5-HT$_{1A}$ monomer was minimized; loops were refined. The stereochemical quality of model was evaluated by Ramachandran Plot and PROCHECK server. More than 90%

of the backbone of dihedral angle residing in favourable region. Model was found to be validated by having more than 94% residues fall under allowed regions without any steric clashes. Rest of the deviations were found to be in region away from binding site. The reliable homology model used in this work was found to be similar as reported in literature.

Three antagonist; *p*-MPPF, BMMP and WAY-100635 were used in the docking studies to understand the binding pose of our ligand with 5-HT_{1A} receptor. To gain insight into the structural understanding of ligand interactions with 5-HT_{1A} receptor, flexible docking has been performed. The docked pose of DO3A-butyl-MPP to the 5-HT_{1A} receptor is the best-energy minimized complex in terms of Glide XP Gscore out of multiple generated clusters. The docking pose of DO3A-butyl-MPP at the shallow antagonist binding pocket of 5-HT_{1A} was found to be high energy with Gscore;-12.132 due to the contribution of hydrophobic residues interactions with the ligand. In the ligand, DO3A-butyl-MPP, the carboxylate groups and carbonyl of cyclic moiety of DOTA is involved in interaction with hydrogen bonding with side chain residues, His376, Gly382, Ile189 and Lys191 (Figure 8a &8b). In addition, π-cation interactions of protonated NH of piprazine moiety with positively charged Asp116 and Phe112. Our results showed a promising results for thermodynamic parameters obtained by docking of the DO3A-butyl-MPP and interactive residue present in the active site of the 5-HT_{1A} receptor. The contribution to thermodynamic parameters includes Lipo, evdw, ecoul and Glide energy terms in the Gscore are -1.457, -43.498, -22.318 and -74.324 respectively. The Lipo term defines contribution from the aromatic hydrophobic residue; Phe361, evdw and coul are van der waal and coulomb energy from carboxylate group of residues in the vicinity of DO3A-butyl-MPP. The XP score has the highest contribution from the Hbond factor (-2.99) due to Asp116 which thus represents the most important interactions for amine group of MPP moiety with 5-HT_{1A} receptors. The Asp116 interactions with azapirones buspirone and sunepitron is well known with piperazine amine as in case of DO3A-butyl-MPP. This binding mode is in general agreement with putative binding modes suggested in a published ligand-supported homology model of 5-HT_{1A} receptor. Also the binding pose is quite consistent with the available experimental studies and importance of these residues are evidenced by site-directed mutagenesis. Form docking pose, the antagonist binding pocket was found to be relatively shallow and involved in various interactions at the site. The antagonist *p*-MPPF is involved in π-π interactions with Phe362 and hydrogen bonding with backbone of Ile189 whereas BMPP is involved in π-π interactions Arg181 and hydrogen bonding with backbone of Ile189. But in case of WAY-100635, one additional π-π interactions with Phe361 was obtained. As

compared to these interactions. DO3A-butyl-MPP was aligned in hydrophobic pocket conserved in all three studied antagonists Glide XP scoring mode in flexible docking has predicted the minimized energy complexes in terms of XP score. The docking pose of DO3A-butyl-MPP at the shallow antagonist binding pocket of $5HT_{1A}$ was found to be high G score of -12.132. The high G score signifies the contribution to G score due to important hydrophobic residues surrounding the ligands.

In addition to the above interactions, the aromatic ring of piperazine moiety of DO3A-butyl-MPP was involved in π-π stacking with Phe361 and Phe362 and hydrogen bond interactions with the side chain of Asp116. The resident binding pocket of both uncomplexed and complexed DO3A-butyl-MPP was found to be conserved and comparable to our pervious results with known antagonists in which docking performed in flexible mode showing appreciable G-score.

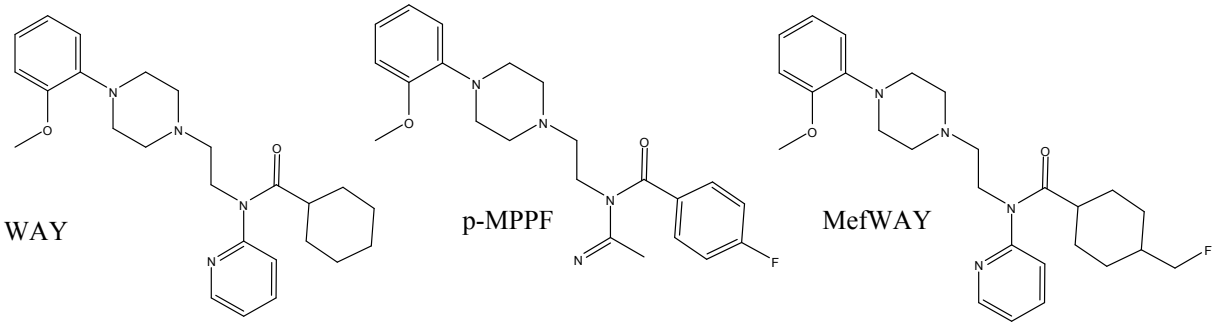

WAY p-MPPF MefWAY

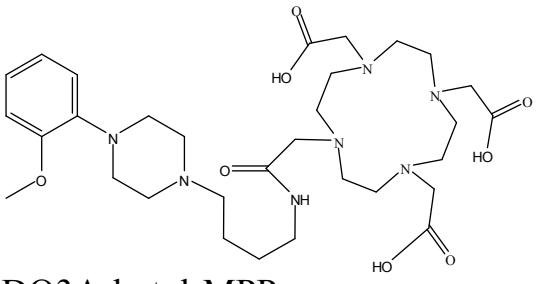

DO3A-butyl-MPP

P-MPPF-Ref

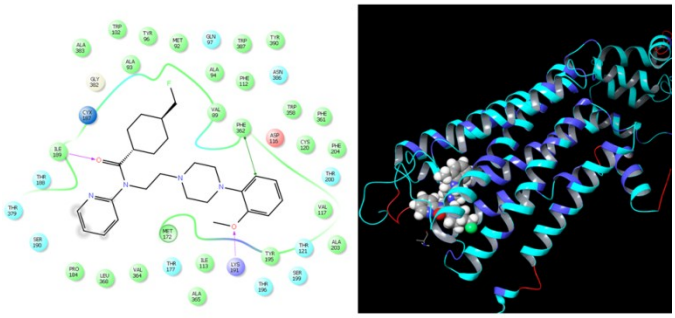

Charged (negative)
Charged (positive)
Polar
Hydrophobic
Glycine
Metal
Water
Hydration site
Displaced hydration site
π-π stacking
π-cation
H-bond (backbone)
H-bond (side chain)
Metal coordination
Solvent exposure

BMPP-Ref

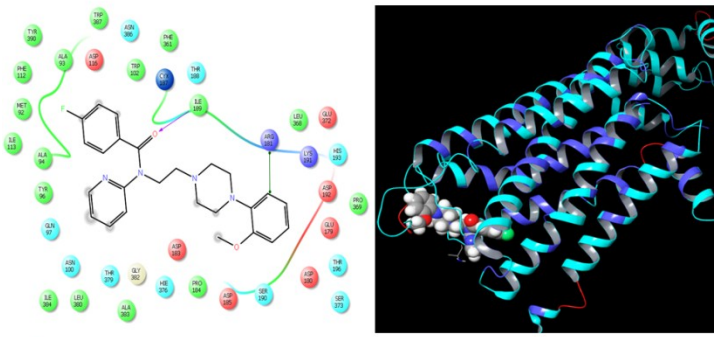

Charged (negative)
Charged (positive)
Polar
Hydrophobic
Glycine
Metal
Water
Hydration site
Displaced hydration site
π-π stacking
π-cation
H-bond (backbone)
H-bond (side chain)
Metal coordination
Solvent exposure

Way 100635

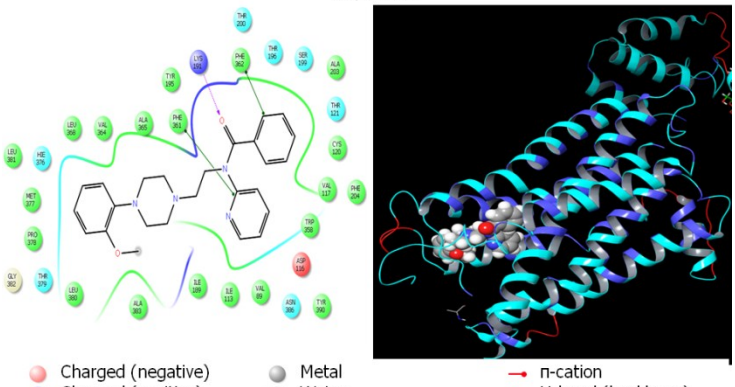

Charged (negative)
Charged (positive)
Polar
Hydrophobic
Glycine
Metal
Water
Hydration site
Displaced hydration site
π-π stacking
π-cation
H-bond (backbone)
H-bond (side chain)
Metal coordination
Solvent exposure